Reducing the Error of Measurement of the Potentiometric Method of the Conductive Liquid Level Meter

Andrey Smirnov
Manash Kozybayev North Kazakhstan University, Petropavlovsk, Kazakhstan
andronio3@gmail.com

Ekaterina Ritter
Manash Kozybayev North Kazakhstan University, Petropavlovsk, Kazakhstan
esritter@ku.edu.kz (corresponding author)

Alexey Savostin
Manash Kozybayev North Kazakhstan University, Petropavlovsk, Kazakhstan
asavostin@ku.edu.kz

Dmitry Ritter
Manash Kozybayev North Kazakhstan University, Petropavlovsk, Kazakhstan
dritter@ku.edu.kz

Andrey Lengard
Manash Kozybayev North Kazakhstan University, Petropavlovsk, Kazakhstan
lengard111@gmail.com

Received: 25 September 2024 | Revised: 12 November 2024 and 24 November 2024 | Accepted: 27 November 2024

 DOI: https://doi.org/10.48084/etasr.9099

ABSTRACT

This article examines the linearization of a nonlinear transfer characteristic in a two-component sensor, with the potentiometric level meter serving as a case study. The conducted analysis employs a method of interpolation involving two interrelated variables: the liquid level readings are contingent upon both the liquid level and the liquid conductivity, while the liquid conductivity readings are influenced by both the liquid conductivity and the liquid level. The objective of the current paper is to identify a mathematical approach that enhances the precision of the measurement. A methodology for linearizing the nonlinear transfer characteristic of a conductivity level meter was established through the integration of two conversion correction tables and piecewise quadratic interpolation with iteration in the form of a table algorithm. This approach resulted in a reduction in the measurement error compared to the interpolation methods without iteration.

Keywords-potentiometric method; conductive liquid level meter; numerical modeling methods; finite element method; measurement error

I. INTRODUCTION

Level sensors are designed to precisely measure the level of liquids within a container, offering invaluable insights into the storage, processing, and distribution of a product. The measurement of liquid levels is of significant importance in production processes, as it allows the determination of the mass and flow rate of liquid products, as well as the control of the mixing ratio [1-3]. This crucial parameter not only guarantees the effective supervision of production operations but also influences the ultimate quality of the final product. To guarantee the production of a superior quality product, it is essential to ensure the precision of the product level measurement. The accurate measurement of product levels allows for the optimization of the production processes, the reduction of raw material and resource losses, and the assurance of their compliance with rigorous regulations and quality standards. This ultimately leads to enhanced plant competitiveness and customer satisfaction, which are pivotal

elements in the contemporary industry. In the filling of dairy products, the accurate determination of the product level in the intermediate tank is of great consequence with respect to the precise dosing of the product. One method of continuous measurement is potentiometry. The potentiometric method dedployed for measuring the level of an electrically conductive liquid has been in use for a considerable period of time [4]. Its principal technical characteristics are outlined in [5-8]. In the event that level gauges are employed, it is imperative that the consumer adhere to all instructions provided with the gauges, including consideration of the potential for additional measurement error in a range of operational contexts. However, the additional errors of the potentiometric level meter remain unknown. In order to identify the additional measurement errors by the level meter, authors in [9, 10] conducted simulations of the liquid level measurement under a variety of application conditions. This article presents evidence that an additional error in measuring the level of a highly conductive liquid by a potentiometric level meter does in fact occur and proposes a method for increasing measurement accuracy.

II. MATERIALS AND METHOD

A. Analyzing the Occurrence of Additional Measurement Error

The operation of a probe in an electrically conductive liquid can be conceptualized as a ladder circuit. As presented in Figure 1, the schematic depicts the flow of currents out of the probe portion of the probe r_{SL}, placed in the electrolyte through the conductive resistors r_L electrolyte. The specific electrical conductivity of a liquid varies considerably, with its values ranging from 0.04 μS/m for distilled water [11] to 2000 μS/m - 42000 μS/m for seawater [12], and up to 30 cm/m for concentrated solutions of alkalis and acids. In the schematic, U_{SL-} is the voltage at the upper extremity of the probe, U_{SL+} is the voltage at the lower portion of the probe situated within the electrolyte, R_{SM} signifies the electrical resistance of the central rod of the probe, R_{SLI}-R_{SLN} are the elements of the probe's electrical resistance within the ladder circuit, and R_{LI}-Y_{LN} are the elements of the electrical resistance of the liquid within the ladder circuit.

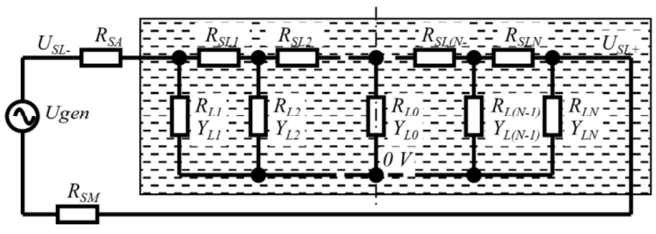

Fig. 1. Schematic diagram of the probe currents.

Although the electrical resistance of the electrolyte (r_L) is considerably greater than that of the probe (r_{SL}), a substantial number of resistors in the electrolyte result in a notable current, which consequently leads to a reduction in the voltage U_{SL+}. This indicates a dependence of the voltage U_{SL+} on the specific conductivity of the liquid (y_L):

$$U_{SL_+} = f(\rho_L) \quad (1)$$

The introduction of this function results in the presence of an additional level of measurement error. The additional error in level measurement, Δam, caused by currents through the electrical resistance of the liquid is shown in Figure 2.

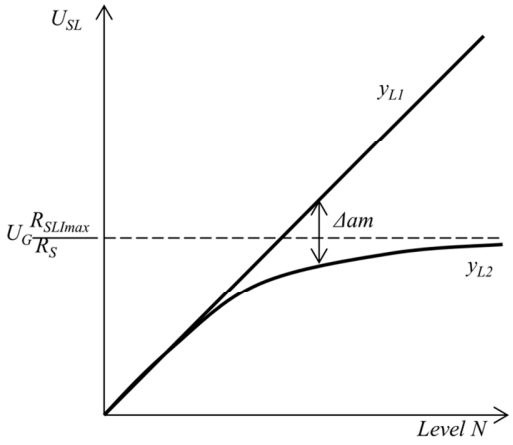

Fig. 2. Approximate dependence of U_{SL} voltage on the probe depth in the electrolyte.

In Figure 2, y_{L1} is the voltage dependence on the probe at a low specific conductivity of the liquid, y_{L2} is the voltage dependence on the probe at a high specific conductivity of the liquid, and Δam is the additional measurement error caused by currents at a high specific conductivity of the liquid. The input electrical resistance R_{SLI} of the probe part, situated within the electrolyte, is defined as a ladder fraction:

$$R_{SLI} = \cfrac{1}{\cfrac{1}{\cfrac{1}{\cfrac{1}{\cfrac{1}{\cfrac{1}{\cfrac{1}{\frac{1}{R_{SL}}+R_L}+R_{SL}}+Y_L}+R_{SL}}+Y_L}+R_{SL}}+Y_L}+R_{SL}} \quad (2)$$

In order to determine the solution of the ladder fraction, it is necessary to begin with the bottom of the fraction and then repeat the division of the fraction. The number of repetitions of the fraction's division is equal to half the number of the links in the ladder chain. The discrete values of the electrolyte level (L), the probe resistance (R_{SL}), and the electrolyte conductivity (Y_L) must be substituted into the error formula:

$$\Delta am = L - L_S = L - L_L \cdot \frac{2R_{SLI}}{2R_{SLI}+R_{SA}} \quad (3)$$

The solution of the ladder fraction by numerical methods is presented in Figure 3 as a graph of additional measurement error. Consequently, the readings obtained from a level gauge are contingent upon two variables: the liquid level and the liquid conductivity. The maximum relative error of the level gauge measurement is equal to σ = 62/900 = 0.069 = 6.9%. In order to calculate the liquid level, it is necessary to measure the conductivity of the liquid in question. The measured conductivity of the liquid is not a linear function of the liquid level, so it becomes evident that it is required to measure and linearize two interdependent parameters, which represents a significant challenge.

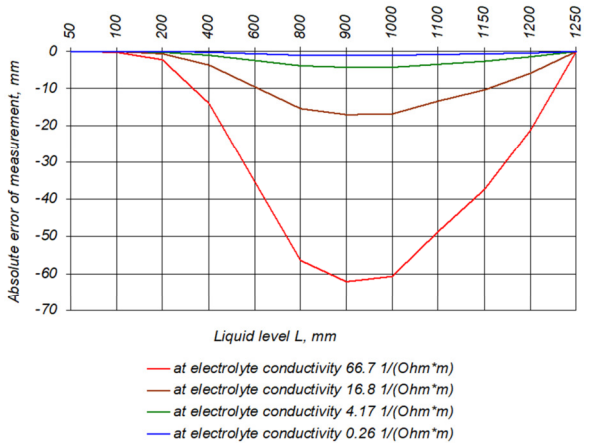

Fig. 3. Dependence of absolute additional error of measurement Δ_{am} on the level and conductivity of the electrolyte.

In instances where the output signal of the sensor is subject to the influence of multiple external factors, its transfer function becomes multi-dimensional. An example of a sensor with a two-dimensional transfer function is an infrared temperature sensor [13]. Consequently, the level probe can be defined as a two-dimensional sensor, representing a combination of a liquid level probe and a liquid conductivity probe.

B. Simulation Method

In order to solve a mathematical model at the micro level, numerical methods based on the discretization of continuous variables are used. In the process of discretization, continuous ranges of value changes are replaced by sets of values at nodal points, which are regarded as nodes within a specific grid. This article employs the finite element method [14-16]. In this context, the electric field in the electrolyte is modeled in a static mode, that is, in a steady state over time. For the purposes of this analysis, it is assumed that the specific electrical conductivity of the electrolyte is constant and identical in all finite elements. A finite element model is to be created, and the electrolyte body is to be divided into equal cubes in Cartesian coordinates. Figure 4 displays the diagram of the potential transfer between the finite elements within the electrolyte. The transfer of potential is shown by arrows, indicating the manner in which it occurs through the contacting faces of adjacent finite elements. The electric field exerts an influence upon the electrolyte, whereby electric currents flow in a direction from areas of higher potential to areas of lower potential, and in a manner perpendicular to the lines of equal potential. This process gives rise to a distribution of electric field potentials within the electrolyte. It is possible to form an equation for the electric currents in the electrolyte using Kirchhoff's law in a specific finite element with coordinates x, y, and z:

$$y_L\left(E_{xy(z+1)} - E_{xyz}\right) + y_L\left(E_{(x-1)yz} - E_{xyz}\right) + \\ +y_L\left(E_{(x+1)yz} - E_{xyz}\right) + y_L\left(E_{xy(z-1)} - E_{xyz}\right) + \\ +y_L\left(E_{x(y+1)z} - E_{xyz}\right) + y_L\left(E_{x(y-1)z} - E_{xyz}\right) = 0 \quad (4)$$

where y_L is the specific electrical conductivity of the electrolyte. Accordingly, the potential of the point of the extreme edge of the finite element, x, y, z, will be calculated as the arithmetic mean of the potentials of the finite elements in contact with the finite element (x, y, z):

$$E_{xyz} = (E_{xy(z+1)} + E_{(x-1)yz} + E_{(x+1)yz} + +E_{xy(z-1)} + \\ E_{x(y+1)z} + E_{x(y-1)z})/6 \quad (5)$$

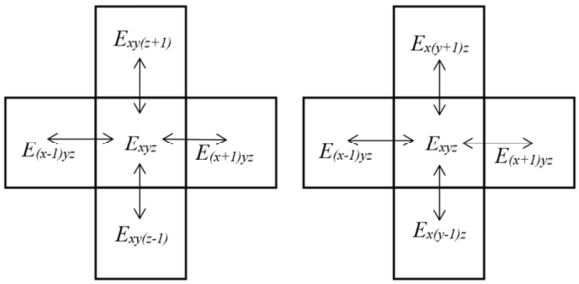

Fig. 4. Diagram of potential transfer between finite elements inside the electrolyte in the vertical and horizontal planes.

The modeling of the electric field in the electrolyte in Cartesian coordinates is a labor-intensive process, as it is necessary to calculate the potentials of the entire set of finite elements. The electrolyte model in Cartesian coordinates will have the form of a parallelepiped of size x, y, z. To ensure the high accuracy of calculations, it is necessary to accept large numbers of x, y, and z. To limit the number of the finite elements, a model of infinite space of finite elements in the faces of the parallelepiped will be constructed by a linear extrapolation in the form:

$$E_{X\infty} = E_{X\infty-1} - (E_{X\infty-2} - E_{X\infty-1}) = 2E_{X\infty-1} - E_{X\infty-2} \quad (6)$$

$$E_{Y\infty} = 2E_{Y\infty-1} - E_{Y\infty-2} \quad (7)$$

$$E_{Z\infty} = 2E_{Z\infty-1} - E_{Z\infty-2} \quad (8)$$

where $E_{X\infty}$, $E_{Y\infty}$, $E_{Z\infty}$ are the potential of the face of the infinite space of finite elements along the axis x, y, z, correspondingly. A numerical model was created to simulate the transfer of the electric potential between discrete elements within the electrolyte. The calculation employs the iteration method, incorporating the boundary conditions within the electrolyte and establishing a connection between the source and the edges of the probe.

C. Analysis of Measurement Error

The level and conductivity probes perform a direct conversion of the measured value, in this case the level and specific conductivity of the electrolyte, into probe measurement signals L_S and y_S, which are subject to some error:

$$L_S = f_{DCL}(L, y_L) \quad (9)$$

$$y_S = f_{DCY}(L, y_L) \quad (10)$$

The level meter and conductometer controller perform an inverse transformation on the probe measurement signals L_S and y_S, yielding output signals of the level and specific conductivity of the electrolyte L_{CALC} and y_{CALC} with a certain degree of error. This yields the approximate relations $L_C \approx L$ and $y_C \approx y_L$. The equations of the inverse transformation are expressed as a system of nonlinear equations:

$$\begin{cases} L_C = f_{BCL}(L, y_L) \cdot f_{DCL}(L, y_L) \cdot L = f_{BCL}(L, y_L) \cdot L_S \\ y_C = f_{BCY}(L, y_L) \cdot f_{DCY}(L, y_L) \cdot y_L = f_{BCY}(L, y_L) \cdot y_S \end{cases} \quad (11)$$

The application of the inverse transformation calculates the correction multipliers to the probe direct transformation function, which, when multiplied together, linearizes the probe transformation function [17-19]. The outcomes of the finite element method numerical modeling within the electrolyte with varying specific conductivity and electrolyte levels, as determined through the iterative finite element potential calculations, are presented in Tables I and II, where $K_L = \frac{L}{L_S}$ and $K_Y = \frac{y_L}{y_S}$. Inverse correction factor tables are generated during the calibration of sensors in experimental and production settings [20].

TABLE I. DEPENDENCE OF THE INVERSE CORRECTION FACTOR OF THE LEVEL MEASUREMENT ON THE PROBE DEPTH IN THE ELECTROLYTE AND THE SPECIFIC CONDUCTIVITY OF THE ELECTROLYTE

		Probe depth in the electrolyte *L*, mm								
	y_L (S/m)	50	100	200	400	800	1.000	1.100	1.150	1.250
Calculated inverse conversion factor of the probe K_L	66.7	1.0053	1.0068	1.0142	1.0389	1.0769	1.0660	1.0484	1.0361	1.0037
	16.8	1.0044	1.0038	1.0047	1.0104	1.0201	1.0175	1.0130	1.0098	1.0012
	4.17	1.0044	1.0030	1.0023	1.0032	1.0054	1.0047	1.0035	1.0027	1.0005
	1.04	1.0041	1.0028	1.0017	1.0014	1.0016	1.0014	1.0011	1.0009	1.0003
	0.26	1.0039	1.0027	1.0016	1.0010	1.0007	1.0006	1.0005	1.0004	1.0003
	0.004	1.0039	1.0027	1.0015	1.0008	1.0004	1.0003	1.0003	1.0003	1.0002

TABLE II. DEPENDENCE OF THE INVERSE TRANSFORMATION COEFFICIENT OF THE SPECIFIC CONDUCTIVITY MEASUREMENT ON THE PROBE DEPTH IN THE ELECTROLYTE AND THE SPECIFIC CONDUCTIVITY OF THE ELECTROLYTE

		Probe depth in the electrolyte *L*, mm								
	y_L (S/m)	50	100	200	400	800	1.000	1.100	1.150	1.250
Calculated inverse conversion factor of the probe K_Y	66.7	0.931	1.044	1.189	1.431	1.797	1.866	1.854	1.832	1.754
	16.8	0.899	0.973	1.035	1.110	1.210	1.231	1.231	1.228	1.214
	4.17	0.883	0.947	0.987	1.019	1.051	1.058	1.058	1.058	1.055
	1.04	0.879	0.940	0.975	0.996	1.011	1.014	1.015	1.015	1.014
	0.26	0.878	0.940	0.972	0.991	1.001	1.004	1.004	1.005	1.005
	0.004	0.877	0.940	0.973	0.991	1.000	1.002	1.003	1.003	1.004

D. Analyzing Data from Inverse Correction Factor Tables

The data from the inverse correction factor Tables I and II were subjected to analysis, which revealed that the inverse correction functions f_{BCL} and f_{BCY} are represented in the tables by discrete inverse correction coefficients of the inverse transformation of the probe/probes K_L and K_Y. This is to say that f_{BCL}= K_L and f_{BCY}= K_Y at the known discrete values L, y_L. The data L, y_L, K_L, and K_Y are organized into matrices for the purpose of visualizing the three-dimensional surfaces of the inverse transformation functions f_{BCL} and f_{BCY}. As illustrated in Figures 5 and 6, the inverse transform functions are represented as interconnected, continuous, and non-monotonic nonlinear functions of two variables.

E. Piecewise Quadratic Interpolation by Power Polynomials with Iteration

The sectors of the three-dimensional surface containing the measurement point from Figures 5 and 6 have been extracted and presented in the separate Figures 7 and 8 for purposes of analysis. The sectors of the three-dimensional surface are defined by curved lines between the interpolation nodes, with nine nodes in total. The inverse correction point of the K_{LS} probe is defined by the coordinates L_S and y_S and is located on the three-dimensional surface of the inverse transformation function f_{BCL}. The probe inverse correction point, K_L, is defined by the coordinates L and y_L and is located on the three-dimensional surface of the inverse transformation function, f_{BCL}. The transition from the point K_{LS} to the point K_L is accomplished through a step-by-step iterative process, as indicated by the arrow.

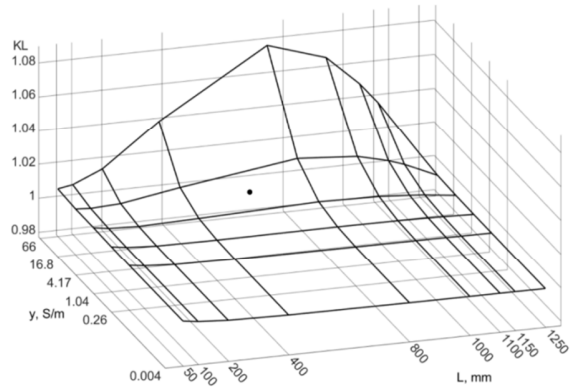

Fig. 5. Three-dimensional surface of the inverse transformation function.

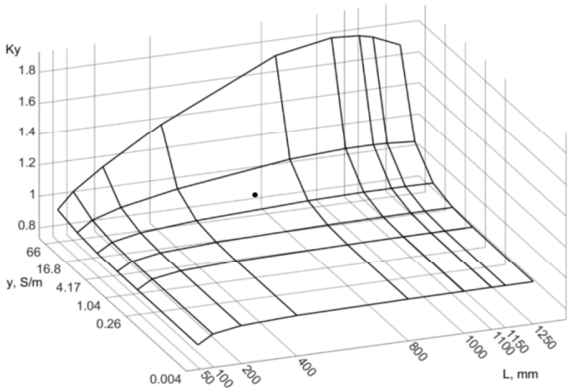

Fig. 6. Three-dimensional surface of the inverse transformation function.

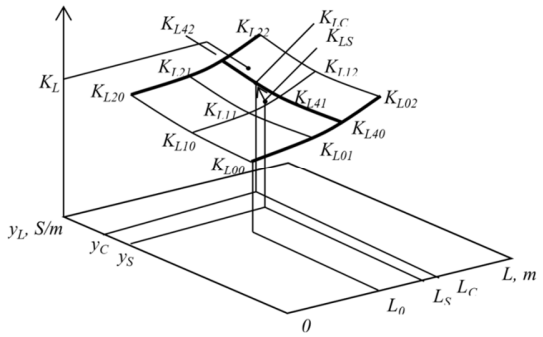

Fig. 7. Selected sectors of the three-dimensional surface of the inverse transformation function.

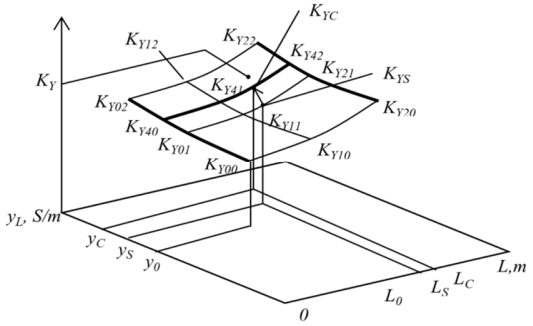

Fig. 8. Selected sectors of the three-dimensional surface of the inverse transformation function.

The inverse transformation function, f_{BCY}, exhibits a comparable structural configuration. The sought point of the inverse correction of the probe K_Y is defined by the coordinates L and y_L and is located on the three-dimensional surface of the inverse transformation function f_{BCY}. The transition from point K_{YS} to point K_Y is accomplished through a step-by-step iterative process in the direction indicated by the arrow. If the function of two variables, f (x, y), is known at the nodes of a two-dimensional rectangular grid, it can be interpolated to any point (x, y). In the first instance, a grid (x_i ... x_n) × (y_i ... y_m) must be interpolated to m points (x, y_i) ... (x, y_m) along the variable x. From the values of the function obtained at these points, one may then proceed to interpolate on the variable y and thereby obtain the value at the point (x, y) [21, 22]. As the interpolating polynomials of several variables are unwieldy, a pragmatic technique is employed: the method of successive interpolation on each variable. Univariate methods are used for this purpose. For the specified sectors of the three-dimensional surface of the function f_{BCL} and f_{BCY}, a sequential two-dimensional interpolation is applied by a second-degree polynomial with a non-uniform grid. Nevertheless, the issue of interpolating the inverse correction coefficients K_L, K_Y cannot be directly addressed, as the probe generates the vectors L_S and y_S, yet fails to produce the unknown vectors L and y_L, which is the object of this study's search. The aforementioned interpolation issue can be addressed through the implementation of numerical techniques, whereby the system of equations pertaining to the K_L and K_Y coefficients can be solved in conjunction with iteration. There is a need to develop a method of interpolation with iteration. Piecewise quadratic interpolation using Newton's second-degree stepped polynomials is conducted to achieve the desired accuracy [23]. The equations of the lines highlighted in the Figures with thickened lines are formulated and solved:

$$\begin{cases} if\ i = 0\ then\ L_X = L_S; y_X = y_S; \\ if\ i > 0\ then\ L_X = K_{LC} \cdot L_S; y_X = K_{YC} \cdot y_S; \\ if\ i < 5\ then\ i = i + 1; \\ \quad else\ L_C = L_X; y_C = y_X; end; \\ K_{L40} = K_{L00} + \delta K_{L011} \cdot (L_X - L_0) \\ \quad +\delta K_{L012} \cdot (L_X - L_0)(L_X - L_1) \\ K_{L41} = K_{L10} + \delta K_{L111} \cdot (L_X - L_0) \\ \quad +\delta K_{L112} \cdot (L_X - L_0)(L_X - L_1) \\ K_{L42} = K_{L20} + \delta K_{L211} \cdot (L_X - L_0) \\ \quad +\delta K_{L212} \cdot (L_X - L_0)(L_X - L_1) \\ K_{LC} = K_{L40} + \delta K_{LY411} \cdot (y_X - y_0) \\ \quad +\delta K_{LY412} \cdot (y_X - y_0)(y_X - y_1) \\ K_{Y40} = K_{Y00} + \delta K_{Y011} \cdot (y_X - y_0) \\ \quad +\delta K_{Y012} \cdot (y_X - y_0)(y_X - y_1) \\ K_{Y41} = K_{Y10} + \delta K_{Y111} \cdot (y_X - y_0) \\ \quad +\delta K_{Y112} \cdot (y_X - y_0)(y_X - y_1) \\ K_{Y42} = K_{Y20} + \delta K_{Y211} \cdot (y_X - y_0) \\ \quad +\delta K_{Y212} \cdot (y_X - y_0)(y_X - y_1) \\ K_{YC} = K_{Y40} + \delta K_{YL411} \cdot (L_X - L_0) \\ \quad +\delta K_{YL412} \cdot (L_X - L_0)(L_X - L_1) \end{cases} \quad (12)$$

where $\delta K_{L012} = \frac{\delta K_{L021} - \delta K_{L020}}{L_2 - L_0}$ are the first separated differences K_L for line 0 of the second order, $\delta K_{LY412} = \frac{\delta K_{LY421} - \delta L_{LY411}}{y_2 - y_0}$ are the first separated differences K_L for line 4 of the second order, $\delta K_{Y012} = \frac{\delta K_{Y021} - \delta K_{Y020}}{y_2 - y_0}$ are the first separated differences K_Y for line 0 of the second order, $\delta K_{YL412} = \frac{\delta K_{YL421} - \delta L_{YL411}}{L_2 - L_0}$ are the first separated differences K_Y for line 4 of the second order. To begin the solution of the equations, it is necessary to identify a known point, L_S and y_S. This can be achieved by replacing L by L_S and y_L by y_S in the equations within the zero-iteration loop. In order to solve the system of equations in the initial and subsequent iteration cycles, it is necessary to replace L_S by L_C and y_S by y_C in the equations, as this will result in the subsequent iteration causing the system of equations to reach equilibrium.

The system of equations in the initial and subsequent iteration cycles will exhibit a tendency for L_X to approach L and for y_X to approach y_L. Upon completion of the designated number of iterations, the results L_X and y_X are written to L_C and y_C, which serve as the sought-after measurement results. The piecewise quadratic interpolation with iteration automatically selects the coefficients of the polynomials for the inverse transform function in both sensor components. The measurement errors for both sensor components are reduced by the accuracy of the initial data and the interpolation method. In order to calculate the value/values using the piecewise quadratic interpolation method with iteration, the original value of the test signal, L = 600, y = 2.5 will be used, which was measured to yield L_S = 598.240, and Y_S = 2.435. Table III presents the initial values for the calculation, while Table IV provides a breakdown of the calculation iterations.

TABLE III. INITIAL DATA FOR THE CALCULATION OF EQUATIONS BY THE PIECEWISE QUADRATIC INTERPOLATION METHOD WITH ITERATION FOR THE MICROCONTROLLER

Coordinates of grid nodes					
L_0	200		y_0	1.04	
L_1	400		y_1	4.17	
L_2	800		y_2	16.8	
Correction coefficients in level meter grid nodes (from Table I)					
K_{L00}	1.00171	K_{L10}	1.00231	K_{L20}	1.00470
K_{L01}	1.00139	K_{L11}	1.00321	K_{L21}	1.01040
K_{L02}	1.00165	K_{L12}	1.00536	K_{L22}	1.02009
Correction coefficients in the conductometer grid nodes (from Table II)					
K_{Y00}	0.97492	K_{Y10}	0.99614	K_{Y20}	1.01093
K_{Y01}	0.98735	K_{Y11}	1.01922	K_{Y21}	1.05112
K_{Y02}	1.03510	K_{Y12}	1.10984	K_{Y22}	1.21038
Calculations of divided differences of the level meter grid (by Newton interpolation)			**Calculations of divided differences of the conductometer grid (by Newton interpolation)**		
δK_{L011}	-0.00000158		δK_{Y011}	0.00397076	
δK_{L021}	0.00000064		δK_{Y021}	0.00378068	
δK_{L012}	0.000000004		δK_{Y012}	-0.00001206	
δK_{L111}	0.00000451		δK_{Y111}	0.00737397	
δK_{L121}	0.00000538		δK_{Y121}	0.00717460	
δK_{L112}	0.000000001		δK_{Y112}	-0.00001265	
δK_{L211}	0.00002849		δK_{Y211}	0.01284015	
δK_{L221}	0.00002422		δK_{Y221}	0.01260969	
δK_{L212}	-0.00000001		δK_{Y212}	-0.00001462	

TABLE IV. CALCULATION OF EQUATIONS BY THE PIECEWISE QUADRATIC INTERPOLATION METHOD WITH ITERATION FOR THE MICROCONTROLLER

Iteration number	**0**	**1**	**2**	**3**	**4**	**5**
K_{L40}	1.00137	1.00137	1.00137	1.00137	1.00137	1.00137
K_{L41}	1.00422	1.00423	1.00423	1.00423	1.00423	1.00423
K_{L42}	1.01549	1.01552	1.01552	1.01552	1.01552	1.01552
δK_{LY411}	0.0009092	0.0009116	0.0009116	0.0009116	0.0009116	0.0009116
δK_{LY421}	0.0008922	0.0008946	0.0008946	0.0008946	0.0008946	0.0008946
δK_{LY412}	-0.00000108	-0.00000108	-0.00000108	-0.00000108	-0.00000108	-0.00000108
K_L	1.002642	1.002696	1.002698	1.002698	1.002698	1.002698
L_c	598.240	599.821	599.853	599.854	599.854	599.854
K_{Y40}	0.98049	0.98071	0.98071	0.98071	0.98071	0.98071
K_{Y41}	1.00646	1.00686	1.00687	1.00687	1.00687	1.00687
K_{Y42}	1.02888	1.02958	1.02960	1.02960	1.02960	1.02960
δK_{YL411}	0.00012985	0.00013078	0.00013081	0.00013081	0.00013081	0.00013081
δK_{YL421}	0.00005604	0.00005679	0.00005681	0.00005682	0.00005682	0.00005682
δK_{YL412}	-0.00000012	-0.00000012	-0.00000012	-0.00000012	-0.00000012	-0.00000012
K_Y	1.02249	1.02314	1.02316	1.02316	1.02316	1.02316
Y_c	2.4350	2.4898	2.4914	2.4914	2.4914	2.4914

III. RESULTS

A. The Linearization Progress

The linearization progress of the two-component level gauge in the process of iteration by steps of calculation repetition is shown in Table V and Figure 9. The level measurement error associated with the piecewise quadratic interpolation method with iteration approaches a limiting value of Δm=-0.146 mm following the second or third iteration step.

TABLE V. PROGRESS OF LINEARIZATION OF THE TWO-COMPONENT LEVEL GAUGE IN THE PROCESS OF ITERATION BY STEPS OF REPETITION OF CALCULATIONS

	Measurement error (mm)					
Iteration step number	0	1	2	3	4	5
Piecewise quadratic interpolation with iteration	1.760	0.179	0.147	0.146	0.146	0.146

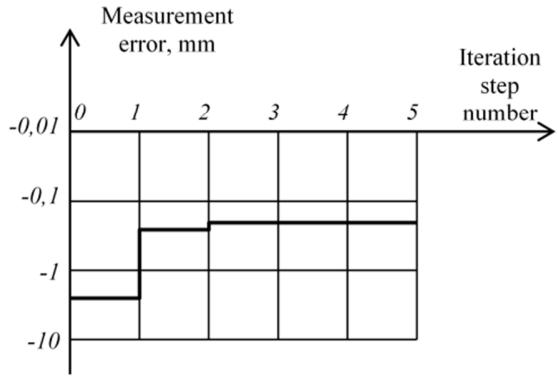

Fig. 9. Progress of linearization of the two-component level gauge in the process of iteration by steps of repetition of calculations.

B. Functional Diagram of a Two-Component Level Gauge with Nonlinearity Correction

In accordance with the proposed method of interpolation with iteration, a functional diagram of a two-component level gauge is developed, integrating the liquid level meter and the conductometer, as portrayed in Figure 10.

In the diagram, B_L is the liquid level probe, which turns a non-electrical value of liquid level L into the voltage L_S. B_Y is the liquid conductivity probe, which turns the non-electrical value of specific conductivity y_L into the voltage y_S. *ADC1* and *ADC2* are the analog-to-digital converters, which convert analog signals L_S and y_S into the digital signals $L_{S\#}$ and $y_{S\#}$. *MUL1* and *MUL2* are the digital signal multipliers, which linearize the nonlinear digital signals $L_{S\#}$ and $y_{S\#}$ into the linear digital signals $L_{C\#}$ and $y_{C\#}$. The digital converters change the analog signals L_S and y_S into the digital signals $L_{S\#}$ and $y_{S\#}$. *DDC1* and *DDC2* are digital-to-digital converters that convert the digital signals $L_{C\#}$ and $y_{C\#}$ into the digital inverse conversion coefficients $K_{Y\#}$ and $K_{L\#}$.

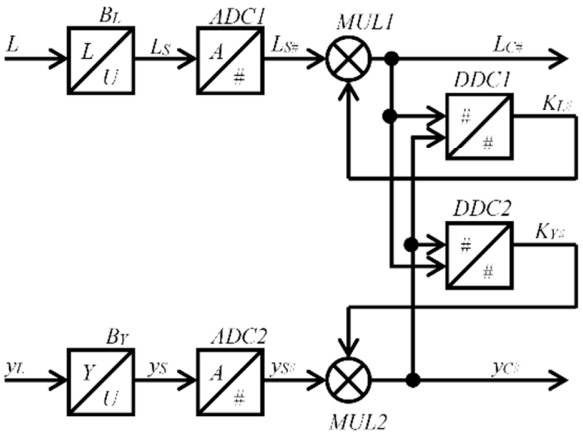

Fig. 10. Functional diagram of the two-component sensor, the combination of the liquid level transmitter, and the conductometer.

C. Stability Analysis of the Two-Component Sensor and Iteration Convergence

The two-component sensor has a functional diagram with closed-loop feedback in the circuit. The MUL1-DDC2-MUL2-DDC1-MUL1 configuration can cause the trigger to be activated or result in unstable positions under certain conditions. The closed-loop feedback is shown in open-loop form in Figure 11, along with the stability conditions.

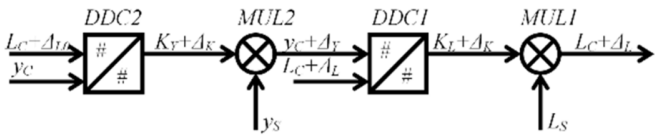

Fig. 11. Functional diagram of open-circuit feedback of a two-dimensional sensor.

In order to calculate the feedback gain of the feedback circuit, it is necessary to provide a small signal L_C in addition to the Δ_{L0} signal. Following this, the transmission of the Δ_{L0} signal through the feedback circuit can be evaluated:

$$\Delta_{K_Y} = \frac{dK_Y}{dL}\Delta_{L_0} \quad (13)$$

$$\Delta_{Y1} = \Delta_{K_Y} y_S = \frac{dK_Y}{dL}\Delta_{L0} y_S \quad (14)$$

$$\Delta_{KL} = \frac{dK_L}{dy}\Delta_{Y1} + \frac{dK_L}{dL}\Delta_{L0} = \frac{dK_L}{dy}\frac{dK_Y}{dL}\Delta_{L0} y_S + \frac{dK_L}{dL}\Delta_{L0} \quad (15)$$

$$\Delta_{L1} = \Delta_{KL} L_S = L_S\left(\frac{dK_L}{dy}\frac{dK_Y}{dL}\Delta_{L0} y_S + \frac{dK_L}{dL}\Delta_{L0}\right) \quad (16)$$

Using the equation of the output signal, the feedback gain K_{BL} is found:

$$K_{BL} = \frac{\Delta_{L1}}{\Delta_{L_0}} = \frac{dK_L}{dy}\frac{dK_Y}{dL} L_S y_S + \frac{dK_L}{dL} L_S \quad (17)$$

In accordance with the Nyquist criterion, the feedback circuit is deemed to be stable when the real part of the K_BL feedback coefficient is less than one. In the KBL feedback coefficient equation, all the numbers are real, indicating that the stability condition is not situated within the complex domain but rather on the real number line:

$$K_{BL} = \frac{dK_L}{dy}\frac{dK_Y}{dL} L_S y_S + \frac{dK_L}{dL} L_S < 1 \quad (18)$$

It is necessary to examine the stability condition of the feedback circuit for the two-component sensor. In order to do so, the derivatives must be substituted in the equation with the first-order Newton polynomial divided differences from Table III:

$$K_{BL} = \delta K_{LY421}\delta K_{YL421} L_S y_S + \delta K_{L021} L_S < 1 \quad (19)$$

Upon substituting the numerical values, the result is:

$$K_{BL} = 0.00089462 \cdot 0.00005682 \cdot 598.240 \cdot 2.435 + 0.00000064 \cdot 598.240 = 0.000456 \ll 1 \quad (20)$$

The feedback gain of the feedback circuit K_{BL} of the two-component sensor is observed to be less than one on numerous occasions. The feedback loop gain value corroborates the convergence property of the iteration in this calculation.

D. Verification of Measurement Error

It is recognized that the minimum deviation of the K_L coefficient calculated by the piecewise interpolation method is situated in proximity to the grid nodes. Consequently, the maximum deviation of the K_L coefficient will be located in the vicinity of the midpoint between the grid nodes. In order to evaluate the accuracy of the piecewise interpolation method with iterations, a test signal was selected from the middle of the interpolation sector, specifically L=600, y_L=2.5. This location is depicted in Figures 6 and 7 as a point. In this instance, L_S (y=2.5, L=600) is equal to 598.24 mm, while y_S (y=2.5, L=600) is equal to 2.435 S/m. The calculations of the errors associated with the method of interpolation with iteration are presented in Table IV. The absolute errors of the method of piecewise quadratic interpolation with iteration are: Δ_L = 599.854 - 600= -0.146 mm, Δ_y = 2.4914 – 2.5 = -0.0086 S/m. The relative errors of the method of piecewise quadratic interpolation with

iteration have a value of: $\sigma_L = \Delta_L/L$ = -0.146/600 = -0.00025, and $\sigma_Y = \Delta_y/y$ = -0.0086/2.5 = -0.0035. Since the inverse transformation functions of the probe K_L and K_Y have descending and ascending regions, we can accept as the result of the numerical simulation for piecewise quadratic interpolation with iteration can be accepted as: $\Delta_L = \pm 0.15$ mm, $\Delta_y = \pm 0.009$ S/m, $\sigma_L = \pm 0.00025$, $\sigma_Y = \pm 0.0035$.

IV. DISCUSSION

Authors in [14] proposed a method of two-dimensional linearization, whereby the coefficients of a surface polynomial are calculated from four systems of equations. In this case, there is no correlation between the values of the second measured value and those of the first value. The two-dimensional polynomial calibration algorithm was tested using the MatLab program, but the calculations are exceedingly complex. The presented interpolation method with iterations is based on the calculation of two interrelated measured values, which are presented in two tables of correction coefficients. The method is performed by calculating one system of equations without an intermediate calculation of the polynomial coefficients. The presented interpolation method with iterations is less costly and can be implemented in an inexpensive general-purpose microcontroller, rather than in a Digital Signal Processor (DSP). The system of (12) is a compiled algorithm for calculating on a microcontroller. It is a relatively straightforward process to develop a program for calculating using a microcontroller. The calculation program comprises two distinct components: a fixed component, and a variable component. Figure 9 shows the manner in which the variable component of the program reduces the measurement error incrementally with the number of calculation iterations. Equation (20) demonstrates the stability of the method and provides numerical evidence in accordance with the Nyquist criterion. The method is verified by a numerical method using a test signal, which is obtained in a manner analogous to that utilized to derive the conversion correction coefficients through the simulation of the field of the level gauge in the electrolyte.

V. CONCLUSIONS

The present article outlines the operational principle of a potentiometric level gauge and provides numerical evidence to substantiate the existence of an additional error in level measurement that arises in the presence of a high specific conductivity of the liquid. The subsequent numerical modeling of the level meter probe in the liquid confirmed the appearance of an additional measurement error of a maximum of 7.7% at a specific electrical conductivity of the liquid, 66.7 S/m, 30% H_2SO_4, and at a liquid level of 0.65 of the probe length. The inverse correction factor for the inverted transformation functions of the potentiometric level meter and conductometer were obtained through the numerical modeling of the level meter probe in liquid. From these inverse correction factor tables, visual representations of the inverse transformation function are obtained through interpolation. The inverse transformation function is presented as a set of interconnected, continuous, non-monotonic, nonlinear functions of two variables. A substantial number of technical publications describe methods for reducing errors through the linearization of inverse transform functions, including both additive and multiplicative approaches. Nevertheless, as the inverse transformation functions of a two-component level meter are nonlinear and interrelated, the problem of interpolating the inverse correction coefficients K_L, K_Y cannot be solved directly. This is because the probe produces the vectors L_S, y_S, but does not provide the vectors L, y_L, which are the unknown variables.

The proposed method of interpolation with iteration, enables the simultaneous numerical interpolation of two variables representing measured quantities. The incorporation of iteration into the process of interpolation calculation has been demonstrated to reduce the measurement error by a factor of seven for piecewise quadratic interpolation. In accordance with the proposed method of interpolation with iteration, a functional diagram of a two-component level meter, which is a combination of a liquid level meter and a liquid conductometer, is constructed. This allows for the composition of an algorithm for calculating the interpolation with iteration by a microcontroller. Additionally, a methodology for analyzing the stability of the two-component sensor was presented, including an equation for determining the stability condition of the two-component level gauge in the presence of a trigger lock or the generation of unstable positions under specific conditions in closed-loop feedback.

ACKNOWLEDGEMENT

This work was supported by the Science Committee of the Ministry of Science and Higher Education of the Republic of Kazakhstan under the Grant number AP13268797.

REFERENCES

[1] P. Mohindru, "Development of liquid level measurement technology: A review," *Flow Measurement and Instrumentation*, vol. 89, Mar. 2023, Art. no. 102295, https://doi.org/10.1016/j.flowmeasinst.2022.102295.

[2] Y. Yan, L. Wang, T. Wang, X. Wang, Y. Hu, and Q. Duan, "Application of soft computing techniques to multiphase flow measurement: A review," *Flow Measurement and Instrumentation*, vol. 60, pp. 30–43, Apr. 2018, https://doi.org/10.1016/j.flowmeasinst.2018.02.017.

[3] Y. Singh, S. K. Raghuwanshi, and S. Kumar, "Review on Liquid-level Measurement and Level Transmitter Using Conventional and Optical Techniques," *IETE Technical Review*, vol. 36, no. 4, pp. 329–340, Jul. 2019, https://doi.org/10.1080/02564602.2018.1471364.

[4] D. Braendle and P. Fend, "Sensor Array for the Potentiometric Measurement of a Fill Level in a Container," BAU 1803 US-PAT.

[5] *"Potentiometric Level Measurement Principle," Inst Tools, Sep. 20, 2017. https://instrumentationtools.com/potentiometric-level-measurement-principle.*

[6] "Rapid response time the potentiometric level measurement from NEGELE," *United Kingdom*. https://www.anderson-negele.com/uk/application/rapid-response-time-potentiometric-level-sensor/

[7] W. Hennessy, "Flow and Level Sensors," in *Sensor Technology Handbook*, J. S. Wilson, Ed. Burlington: Newnes, 2005, pp. 237–254.

[8] Z. Berk, *Food Process Engineering and Technology*. Academic Press, 2018.

[9] A. Smirnov, E. Ritter, A. Savostin, D. Ritter, and S. Moldakhmetov, "Modeling of a Potentiometric Level Meter in a Heterogeneous Liquid and Error Assessment," *Bulletin of Kazatk*, vol. 130, no. 1, pp. 404–413, 2024, https://doi.org/10.52167/1609-1817-2024-130-1-404-413.

[10] A. P. Smirnov, E. S. Ritter, A. Savostin, D. Ritter, and S. Moldakhmetov, "Numerical simulation of a potentiometric level meter in an electrically conductive medium and improving the level meter construction," *Toraighyrov University*, vol. 4, 2013, https://doi.org/10.48081/YYOH8649.

[11] A. Gapparov and M. Isakova, "Study on the characteristics of water resources through electrical conductivity: A case study of Uzbekistan," *IOP Conference Series: Earth and Environmental Science*, vol. 1142, no. 1, Mar. 2023, Art. no. 012057, https://doi.org/10.1088/1755-1315/1142/1/012057.

[12] V. H. McNeil and M. E. Cox, "Relationship between conductivity and analysed composition in a large set of natural surface-water samples, Queensland, Australia," *Environmental Geology*, vol. 39, no. 12, pp. 1325–1333, Nov. 2000, https://doi.org/10.1007/s002549900033.

[13] J. Fraden, *Handbook of Modern Sensors: Physics, Designs, and Applications*. London, UK: Springer International Publishing, 2015.

[14] D. G. Pavlou, "An Overview of the Finite Element Method," in *Essentials of the Finite Element Method*, D. G. Pavlou, Ed. Stavanger, Norway: Academic Press, 2015, pp. 1–18.

[15] C. M. Tan, W. Li, and Z. Gan, "Applications of finite element methods for reliability study of ULSI interconnections," *Microelectronics Reliability*, vol. 52, no. 8, pp. 1539–1545, Aug. 2012, https://doi.org/10.1016/j.microrel.2011.09.015.

[16] A. Popa, M.-G. Manea, and M.-V. Ristea-Komornicki, "FEM Structural Analysis for Ship's Beam Modification: A Case Study," *Engineering, Technology & Applied Science Research*, vol. 14, no. 4, pp. 15848–15853, Aug. 2024, https://doi.org/10.48084/etasr.7885.

[17] G. Horn and J. L. Huijsing, *Integrated Smart Sensors*. Boston, MA, USA: Springer US, 1998.

[18] P. Pasic, "Generalised sensor linearisation and calibration, "M.S. thesis, Dublin City University, Dublin, Ireland, 2004.

[19] M. B. Marinov *et al.*, "Linear Interval Approximation of Sensor Characteristics with Inflection Points," *Sensors*, vol. 23, no. 6, Jan. 2023, Art. no. 2933, https://doi.org/10.3390/s23062933.

[20] L. E. Bengtsson, "Lookup Table Optimization for Sensor Linearization in Small Embedded Systems," *Journal of Sensor Technology*, vol. 2, no. 4, pp. 177–184, Dec. 2012, https://doi.org/10.4236/jst.2012.24025.

[21] M. Gasca and T. Sauer, "Polynomial interpolation in several variables," *Advances in Computational Mathematics*, vol. 12, no. 4, pp. 377–410, Mar. 2000, https://doi.org/10.1023/A:1018981505752.

[22] B. D. Bojanov, H. A. Hakopian, and A. A. Sahakian, *Spline Functions and Multivariate Interpolations*. Dordrecht, Netherlands: Springer Netherlands, 1993.

[23] J. Stoer and R. Bulirsch, "Interpolation," in *Introduction to Numerical Analysis*, J. Stoer and R. Bulirsch, Eds. New York, NY: Springer, 2002, pp. 37–144.